

# Formation and Structure of High Mechanical Performance Fibers. II. Flexible Polymers

TAKESHI KIKUTANI

Department of Organic and Polymeric Materials, Graduate School of Science and Engineering,  
Tokyo Institute of Technology, Tokyo, Japan

*Received 8 November 2000; accepted 18 November 2000*

**ABSTRACT:** Conditions for the formation of high performance fibers from flexible and semi-flexible polymers are reviewed in terms of the chemical structure, chain conformation, super structure, and modeling. Small cross-sectional area and extended conformation are important factors for designing the high-performance polymers. Tensile modulus decreases significantly by only a small contraction of main chain from the planar zigzag conformation. Model calculation for the estimation of the ultimate tensile strength includes the evaluations of bond strength and the kinetic theory for rupture of primary and secondary bonds. Presence of defects such as chain ends are also considered. Macroscopic defects can be evaluated based on Griffith's theory. Drawability, which is important for the production of high performance fibers, can be improved through the control of entanglement. Experimental and industrial procedures for the production of high performance fibers such as gel spinning of polyethylene, pressurized drawing of polyoxymethylene, controlled shrinkage and drawing of polytetrafluoroethylene, and solid state co-extrusion of high molecular weight poly(ethylene terephthalate) are also reviewed. © 2002 John Wiley & Sons, Inc. *J Appl Polym Sci* 83: 559–571, 2002

**Key words:** tensile modulus; tensile strength; drawing; defect; entanglement

## INTRODUCTION

Although the first commercial synthetic fiber, polyamide 66, was advertised as the fiber stronger than steel (if the strength is compared using the unit of gram-force per denier), it seems that systematic research on the development of high-performance fibers from flexible polymers only started in the 1970s. Since then, intensive studies for the development of new techniques and refinement of each process have been accomplished by many researchers all over the world. Along with the experimental approaches for the improvement of mechanical properties, there were theoretical developments on the ultimate mechanical

properties of fibers. Development of computer simulation techniques played a significant role for these analyses.

## BASIC CONCEPT FOR THE PRODUCTION OF HIGH-PERFORMANCE FIBERS FROM FLEXIBLE POLYMERS

### Ultimate Tensile Modulus and Strength

One of the most important characteristics of polymeric materials is their anisotropic property. The anisotropy arises from the difference in the binding energies between atoms, in that the covalent bond in the molecular chain is about  $500\times$  stronger than the van der Waals interaction. Therefore, the ultimate mechanical properties of fibers can be obtained only when the covalent bond is

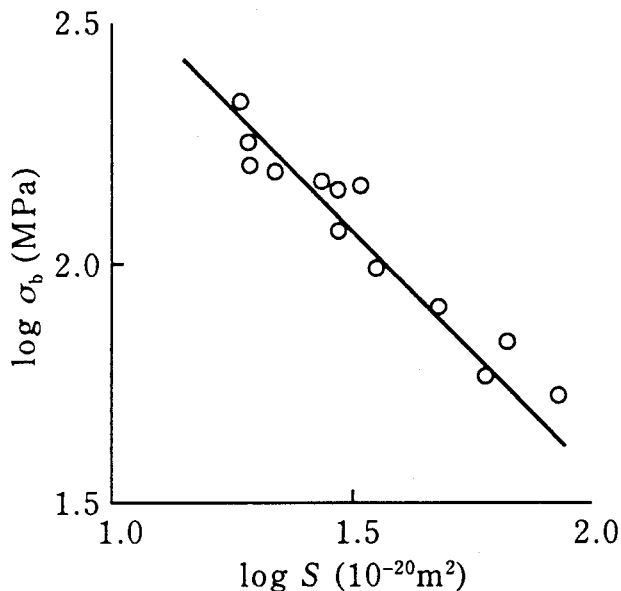
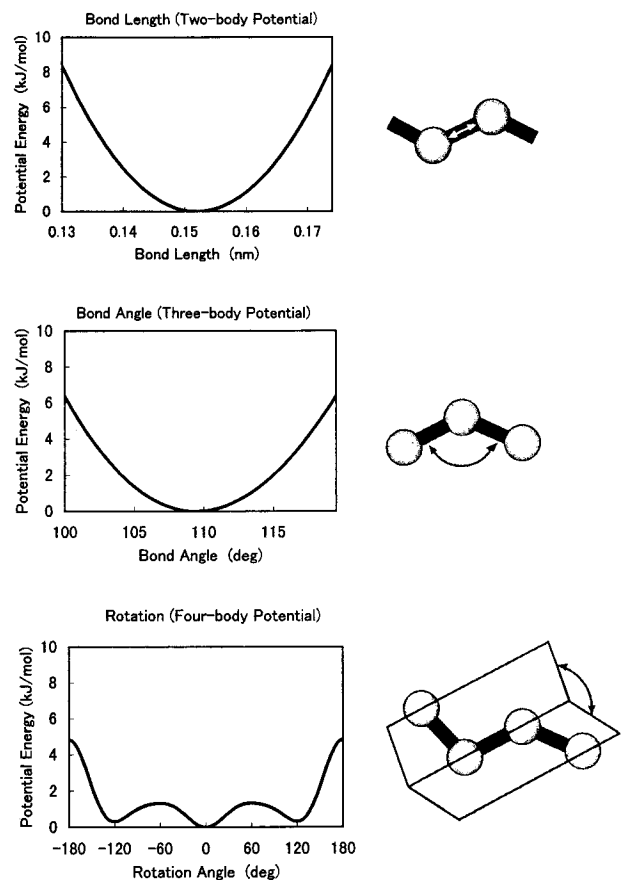
**Table I** Dependence of Theoretical Strength and Modulus on Cross-Sectional Area of Single Molecular Chain for Various Polymers

Polymer	Cross-sectional Area per Single Chain (nm <sup>2</sup> )	Theoretical Strength (gf/d)	Theoretical Modulus (gf/d)
PE	0.193	372	2775
PP	0.348	218	423
PA6	0.192	316	1406
PVA	0.228	236	2251
PET	0.217	232	1500
PAN	0.304	196	833

fully utilized. In other words, to obtain the ultimate mechanical properties, all the molecules in the fiber must be perfectly oriented in the direction of the fiber axis.

The chemical structure of polymers also has significant influence on the ultimate mechanical properties. There are three important factors for the designing of high-performance polymers from the viewpoint of chemical structure: 1. small cross-sectional area per chain, 2. extended chain conformation, and 3. strong chemical bond in main chain. The importance of these factors can be easily explained by comparing the chemical structures of polyethylene (PE) and polypropylene (PP). The chemical structure of PP can be constructed by simply replacing one hydrogen

atom in PE by the methyl group. Because of the enlargement of the side-group, the PP chain should have a larger cross-sectional area than PE. Along with this, conformation of molecules changes from planar zigzag of PE to 3/1 helix of PP. Eventually, PE has much superior ultimate mechanical properties than PP. Cross-sectional

**Figure 1** Relationship between fiber strength  $\sigma_b$  and cross-sectional area of single chain  $S$ .<sup>1</sup>**Figure 2** Two-, three-, and four-body intermolecular potentials for polymethylene.

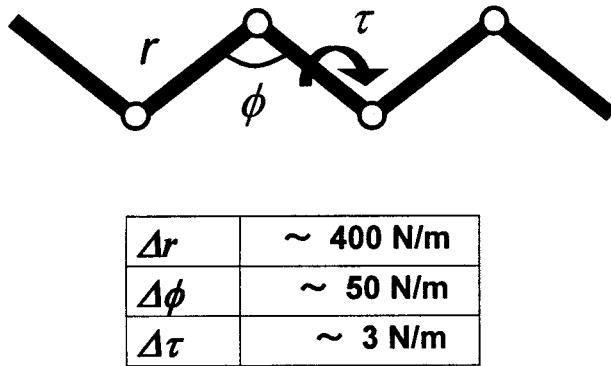


**Figure 3** Elastic constant for various modes of bond displacement.

area, theoretical strength, and modulus of various flexible polymers are summarized in Table I.<sup>1</sup> Dependence of fiber strength on the cross-sectional area is also plotted in Figure 1.<sup>2</sup>

#### Tensile Modulus

The theoretical estimations of the conformation and mechanical properties of polymeric molecules

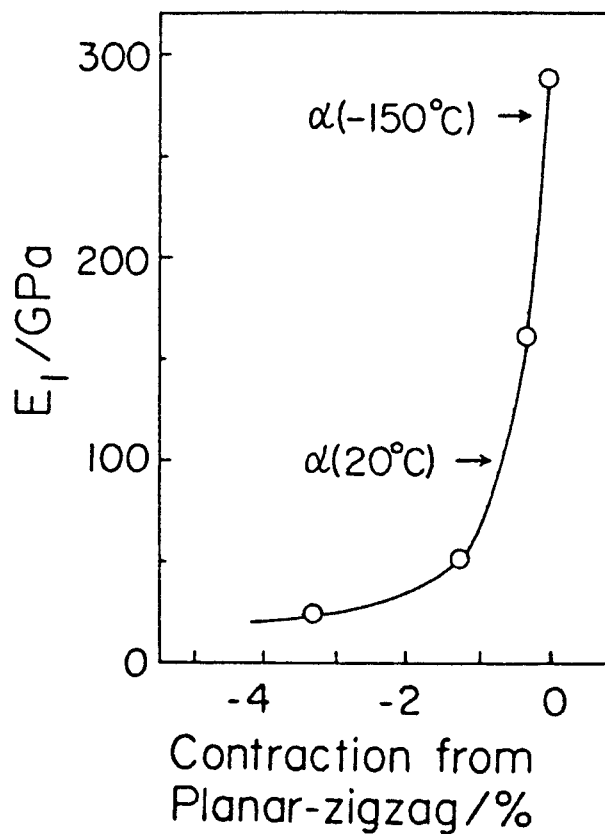


**Figure 4** Tensile modulus versus chain contraction from planar zigzag conformation for polyamide 6 single molecule.<sup>4</sup>

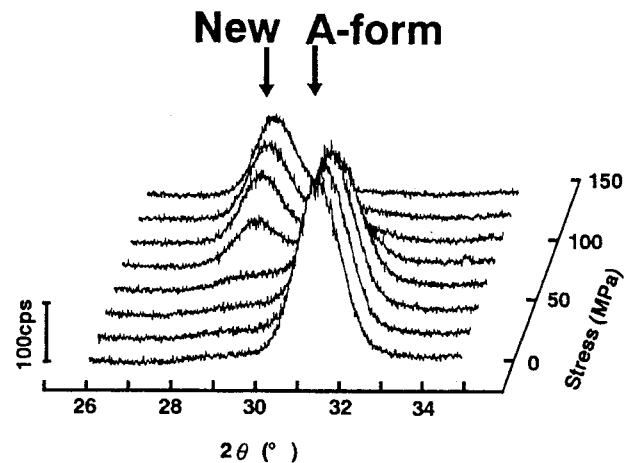


**Figure 5** Variation of meridional wide-angle X-ray diffraction profiles of poly(butylene naphthalate) fibers under tensile stress.<sup>5</sup>

are based on their intramolecular and intermolecular potential energies. For example, effects of the changes of bond length, bond angle, and rotation angle on the potential energy for polymethylene are shown in Figure 2.<sup>3</sup> From these changes in potential energy, elastic constants (force per displacement) can be obtained (Fig. 3). It can be easily recognized from this result that the chain length can be extended easily if the bond rotation occurs under tensile load. Conformations of polyamide 6 (PA6) molecules in  $\alpha$ - and  $\gamma$ -form crystals were investigated by Tashiro and Tadokoro<sup>4</sup> by utilizing the mechanics of crystal lattice theory. It was revealed that in  $\alpha$ -form crystals at room temperature, there is about 1% contraction of the PA6 molecule with respect to the fully extended planar zigzag conformation. This small contraction leads to about 75% reduction of the theoretical tensile modulus. At low temperatures, because of the extension of the PA6 molecule, the tensile modulus was calculated to reach about 300 GPa (Fig. 4).

There are several methods for the measurement of the elastic constants of polymer crystals. One of these is the wide-angle X-ray diffraction method, in which changes of crystal lattice parameters with increasing tensile load are measured from the peak shift of corresponding crystalline reflections. For example, the result of measurement for the poly(butylene naphthalate) reported by Nishino et al.<sup>5</sup> is shown in Figure 5. It can be seen from the figure that  $(105)$  reflection of A-form crystal shifts toward lower diffraction angles with increasing tensile stress, and when the

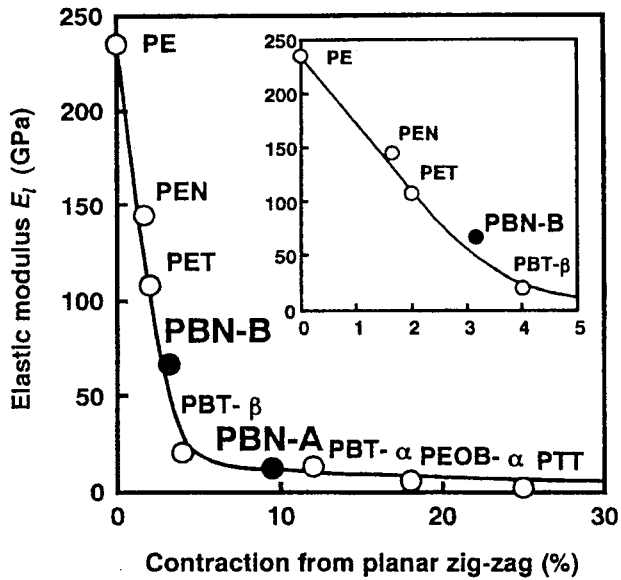


**Figure 6** Relation between tensile elastic modulus and the chain contraction from planar zigzag conformation for aromatic polyesters.<sup>5</sup>

tensile stress exceeds 60 MPa, there is an appearance of a new crystalline peak indicating the change in crystal structure. They also pointed out that there is a universal relationship between the measured tensile modulus and the amount of chain contraction from the planar zigzag conformation (Fig. 6). This result, along with the result shown in Figure 4, suggests that the perfect extension of the main-chain is crucial for the production of high-performance fibers.

### Tensile Strength

Theoretical estimation of tensile strength is more complicated than the tensile modulus. Whereas tensile modulus reflects the average of the structure, tensile strength relates more to the weakest portion in the structure. Strength of a single chemical bond can be calculated from the knowledge of potential energy and the activation volume. More recently, theory of quantum chemistry was applied for the estimation of the strength of molecular chain. Figure 7 shows the changes in the heat of formation and stress of polymethylene chain with increasing strain calculated using the semi-empirical molecular orbital theory.<sup>6</sup> The fracture of the main chain occurred at the strain of 46%. Stress-versus-strain curve was obtained by the differentiation of the heat of formation-versus-strain curve. Bond strength estimated from the maximum stress is about 45 GPa.

### Effects of Defects and Unevenness

A computer simulation model based on the kinetic theory of fracture was developed by Termonia et al.<sup>7</sup> In the theory, rate of a breakage of a bond is assumed to increase with the applied stress. Primary and secondary bonds, which correspond to the covalent bond and to the van der Waals force respectively, are considered. The chain ends are also introduced to the model considering the molecular weight of the polymer. Figure 8 summarizes the model and the result of the calculation. The obtained stress-strain curves for various molecular weights are shown in Figure 9. The strength, defined as the maximum stress in the stress-strain curve, increased with increasing

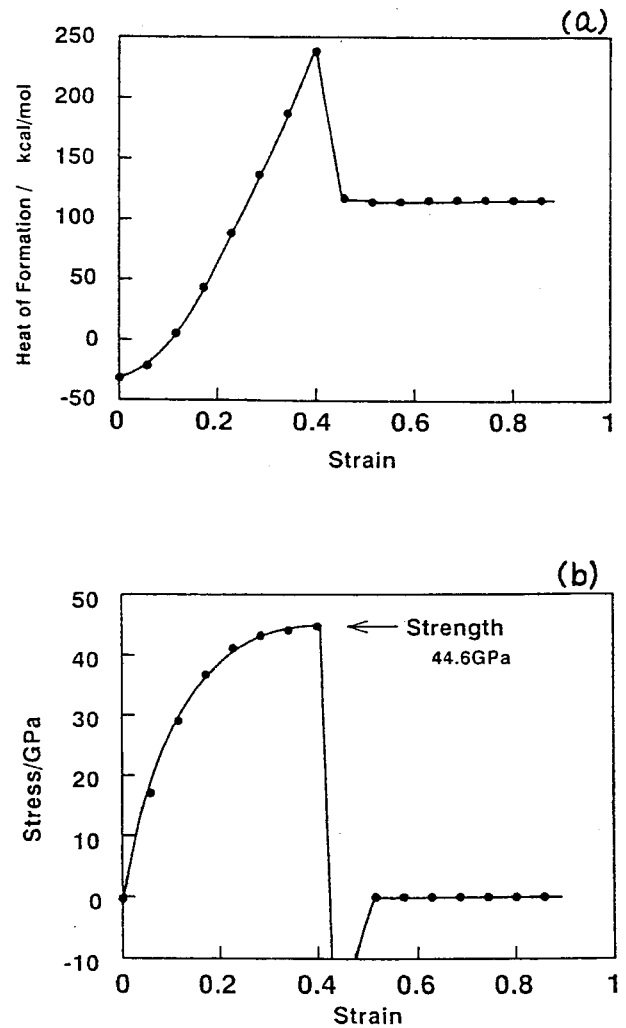


**Figure 7** Tensile deformation and fracture of polymethylene single molecule calculated using semi-empirical molecular orbital method (PM3).<sup>6</sup>

$$v_i = \tau \exp\left[\frac{-U + \beta\sigma}{kT}\right]$$

- $v_i$  rate of a breakage of a bond
- $\tau$  thermal vibration frequency
- $U$  the activation energy of the bond
- $\sigma$  local stress
- $\beta$  activation volume

Primary bond  
 $K_1 = 300 \text{ GPa}$ ,  
 $U_1 = 25 \text{ kcal/mol}$ ,  $\beta_1 = 1.54 \text{ \AA}^3$

Secondary bond  
 $K_2 = 3 \text{ GPa}$   
 $U_2 = 0.65 \text{ kcal/mol}$ ,  $\beta_2 = 2.5 \text{ \AA}^3$

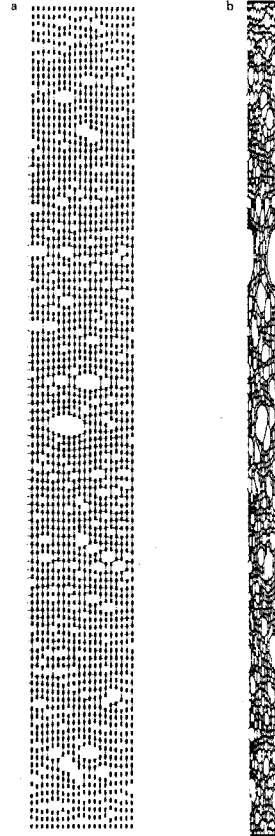
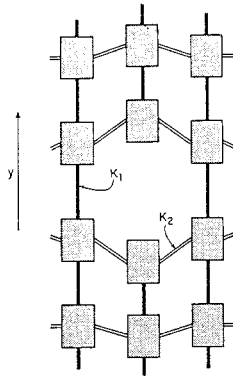


**Figure 8** Model and result of calculation of kinetic theory of fracture proposed by Termonia et al.<sup>7</sup>

molecular weight, and the ultimate strength of ca. 10 GPa was obtained for the molecular weight of 3 million.

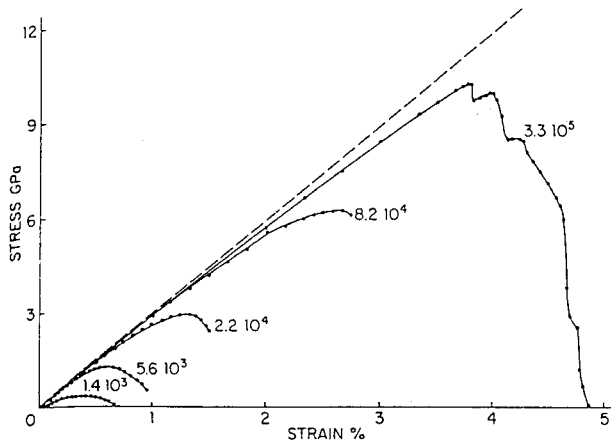


**Figure 9** Calculated stress–strain curves for PE of various molecular weights.<sup>7</sup>

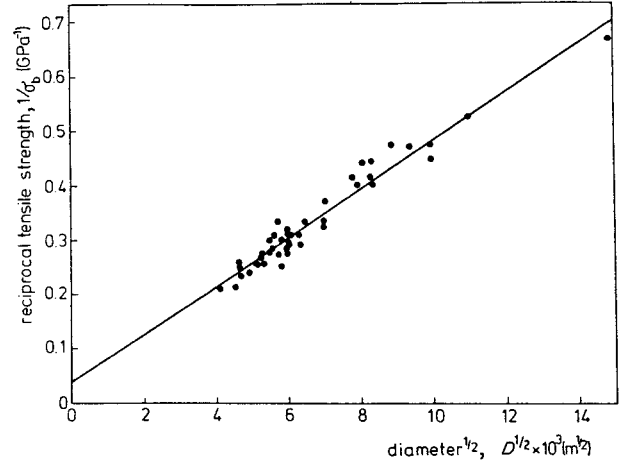


**Figure 10** Dependence of tensile strength  $\sigma_b$  on fiber diameter  $D$  for highly drawn ultrahigh molecular weight PE.<sup>9</sup>

Based on the fracture mechanics, Griffith's theory was applied for the estimation of ultimate strength. The estimated value varied from 10 to 70 GPa, depending on adopted parameters.<sup>8</sup> The Griffith theory was also applied for the estimation of the fiber diameter dependence of tensile strength of high-performance PE fibers.<sup>9</sup> In this analysis, fiber diameter is regarded to have the same effect as the size of the crack. The strength of PE fibers was found to be inversely proportional to the square root of its diameter (Fig. 10),

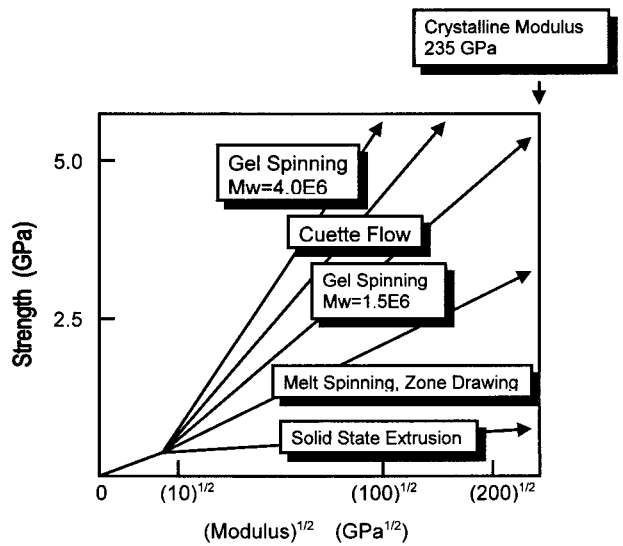


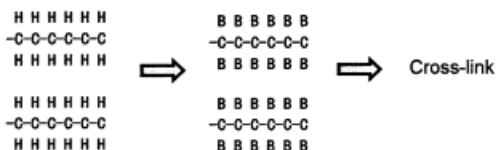
**Figure 11** Relationship between strength and square root of modulus for PE fibers prepared through various drawing processes.<sup>10</sup>

and by extrapolating the straight line to zero, the ultimate strength of 26 GPa was obtained. The fiber strength is determined by the lateral bond strength. This conclusion is based on the analyzed activation energy in fracture process. The obtained value 60–75 kJ/mol is significantly lower than the bond energy of C—C, which is about 300 kJ/mol; and also lower than the value of 113 kJ/mol, which corresponds to the dissociation energy of PE under tensile stress.

Griffith's theory also can be applied for the estimation of the amount of defects (Fig. 11). By plotting the relation between strength and square root of modulus, the gel spinning provides fibers with a smaller number of defects in comparison with solid state extrusion, melt spinning, and zone drawing processes.<sup>10</sup>

#### Future Work: Molecular Design

Through fundamental knowledge on the ultimate modulus and strength of polymers, one can design new polymers that are supposed to have significantly high mechanical properties. An extreme example of the designing of a new polymer is shown in Figure 12, in which all the hydrogen



**E=600 GPa in all the directions**

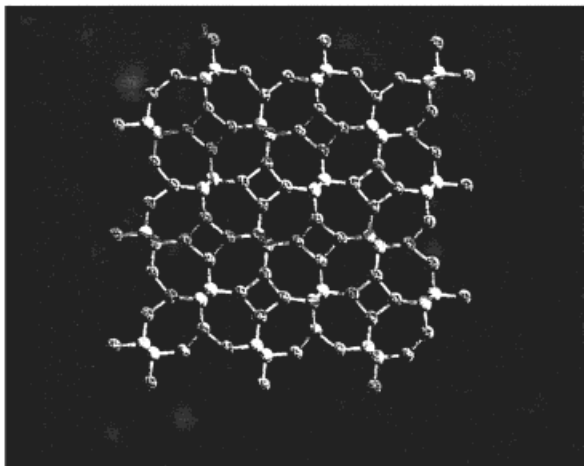


**Figure 12** Computer-designed high-strength molecule based on PE.<sup>11</sup>

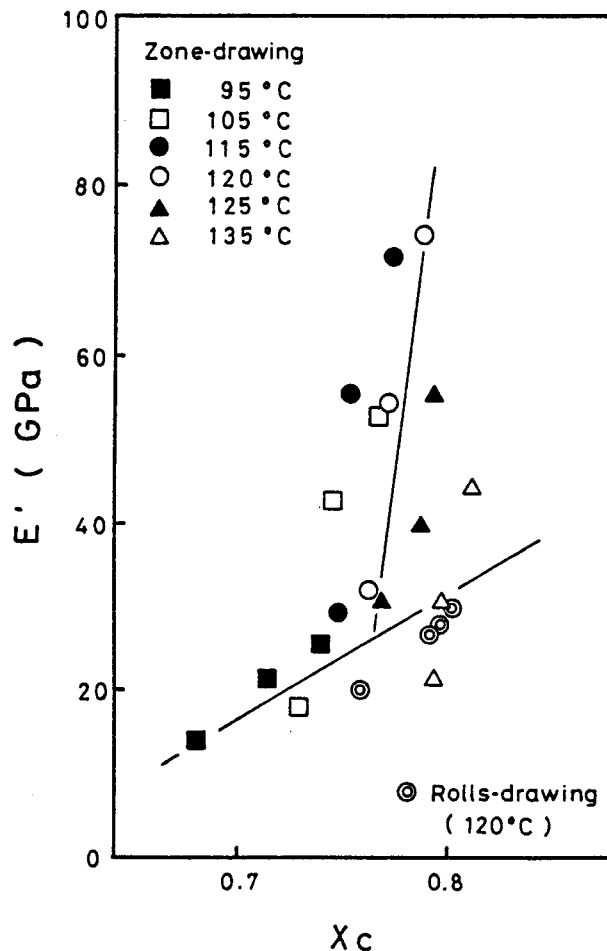


**Figure 13** Dependence of tensile modulus  $E'$  on crystallinity  $X_c$  for PE fibers prepared by zone-drawing process.<sup>12</sup>

atoms in PE are replaced by boron atoms; and then intermolecular crosslinks are made by the chemical bond between boron atoms. This three-dimensionally constructed molecule was analyzed to have tensile modulus of 600 GPa in all directions.<sup>11</sup>

#### Control of Super Structure

If flexible polymers are used for the production of high-performance fibers, the fiber should be crystallized to maintain the extended chain conformation. The ultimate properties are expected to be realized if the crystallinity of the fiber is 100%. In practice, we only can have partially crystallized fibers. If the two-phase model of crystal and amorphous phases is considered, it is important that the parallel model gives much higher mechanical



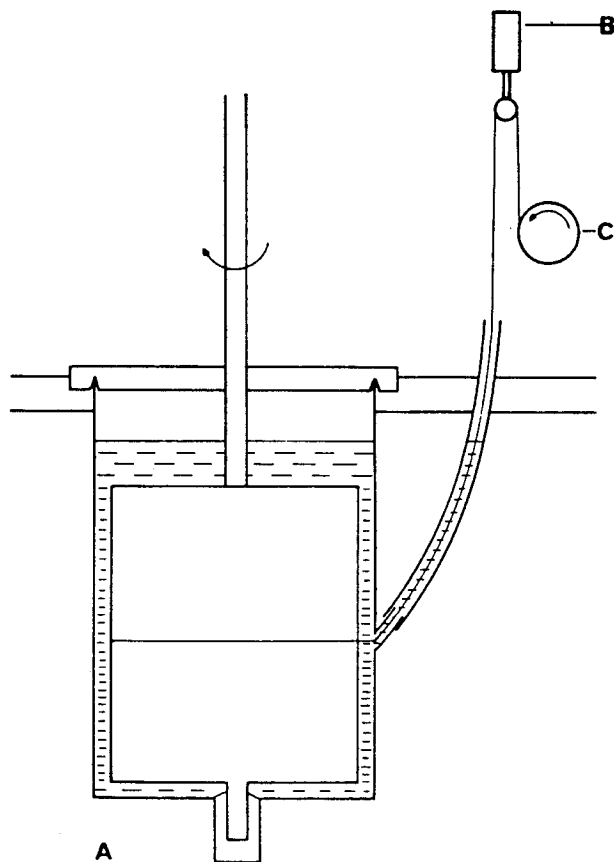


**Figure 14** Couette-flow apparatus for continuous growth of PE fibers from dilute *p*-xylene solution.<sup>13</sup>

properties than the series model, even though the volume fraction of the crystalline phase is the same. In the parallel model, the continuity of extended molecules in the direction of fiber axis is the most important characteristic. In this sense, the construction of continuous crystalline phase, an increase in the amount of so-called taut-tie molecules, and the construction of a shish-kebab structure seems to be an effective method to obtain high-performance fibers.

Figure 13 shows the change of tensile modulus of drawn PE fibers prepared by the zone drawing process.<sup>12</sup> The tensile modulus started to increase abruptly at the crystallinity of 0.77. It was explained that the abrupt modulus increase corresponds to the formation of the continuous crystalline phase.

Figure 14 shows the schematic diagram of the couette apparatus for continuous growth of PE microfibrils from dilute *p*-xylene solutions.<sup>13</sup> A transmission electron micrograph of obtained fibers revealed that the fibers have a shish-kebab

structure. Because of the presence of shish, in which extended PE molecules are continuously aligned in the direction of the fiber axis, the fiber shows significantly high mechanical properties.

#### *Drawability and Efficiency of Drawing*

The drawing process is indispensable for the construction of a highly oriented and extended molecular structure. Basically, there are two types of drawing processes. In cases of highly crystalline polymers like PE or PP, the crystalline structure can be drawn to form a highly oriented crystalline structure. However, in cases of relatively rigid molecules with its glass transition temperature higher than room temperature like polyethylene terephthalate (PET), starting materials for the drawing process usually have an amorphous structure. In both cases, drawability and efficiency of drawing are the key factors for the formation of high-performance fibers.

Okui and Sakai<sup>14</sup> pointed out that the monomer unit length is one of the most important factors for the development of three-dimensionally and highly ordered structure. They explained that the longer the unit length  $d$ , the unit length translation parallel to the chain axis needs the

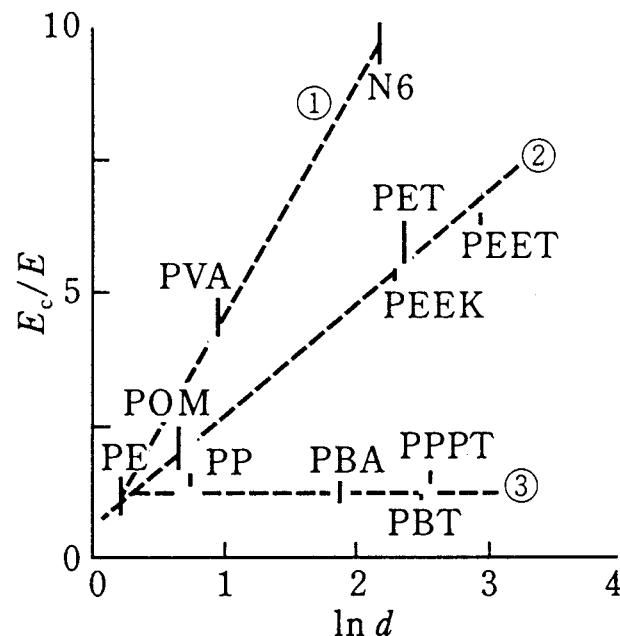


**Figure 15** Relationship between the ratio of the axial crystalline modulus  $E_c$  to the ultimate Young's modulus of produced fibers and the logarithm of the unit length  $d$ .<sup>14</sup>

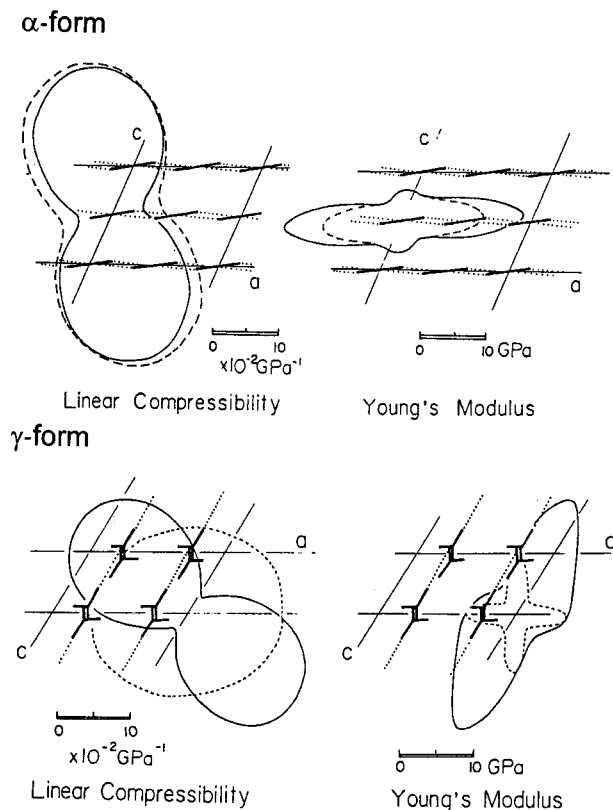


**Figure 16** Effect of intermolecular van der Waals interactions and hydrogen bonds on the mechanical anisotropy of  $\alpha$ - and  $\gamma$ -form polyamide 6 crystals. The solid lines and broken lines represent the calculated results with and without the consideration of hydrogen bond.<sup>15</sup>

longer distances to generate a crystalline packing finding a set of nearest lattice points. The plot of  $E_c/E$  versus  $\ln d$ , where  $E_c$  and  $E$  are the theoretical modulus and the experimentally obtained highest modulus, shows that the polymers can be categorized into three groups (Fig. 15). The highest slope in the plot is for the group of flexible polymers with hydrogen bonds. In this case, the hydrogen bond also prevents the free movement of molecules to find an appropriate position; and it is quite difficult to develop fibers that have a modulus close to the theoretical value. The second-highest slope is for the group of flexible polymers. However, there is no effect of monomer unit length on the tensile modulus in the case of rigid polymers.

The effect of the hydrogen bond on the mechanical properties of PA6 crystals is shown in Figure 16.<sup>15</sup> Linear compressibility is lower and Young's modulus is higher in the direction of hydrogen

bond in both  $\alpha$ - and  $\gamma$ -form crystals. For PA6, it was reported that the crystal modification changes from  $\alpha$ -form to  $\gamma$ -form by the treatment in iodine-potassium iodide aqueous solution.<sup>16</sup> The plastic deformation behavior of crystals is reported to change significantly with the change in crystalline structure.<sup>17</sup>

### Control of Entanglement

The drawability and the efficiency of drawing are influenced by entanglement. Many techniques for the improvement of drawability have been developed, based on the concept of the control of the entanglement structure. It was reported by Pawlikowski et al.<sup>18</sup> that the compacted reactor powder of ultrahigh molecular weight PE can be drawn up to the draw ratio of about 60 and exhibit relatively high mechanical properties. Certain nascent polymers have unusual thermal and morphological properties that are irretrievably lost once the polymer has been melted. The amount of entanglement in the reactor powder is much smaller than the polymer that experienced the molten state. The use of reactor powder has a potential for direct processing without prior solvent or thermal treatments.

It is well known that polymer molecules are aligned perpendicular to the surface of a single crystal prepared from a dilute solution. Therefore, in a single-crystal mat prepared by stacking

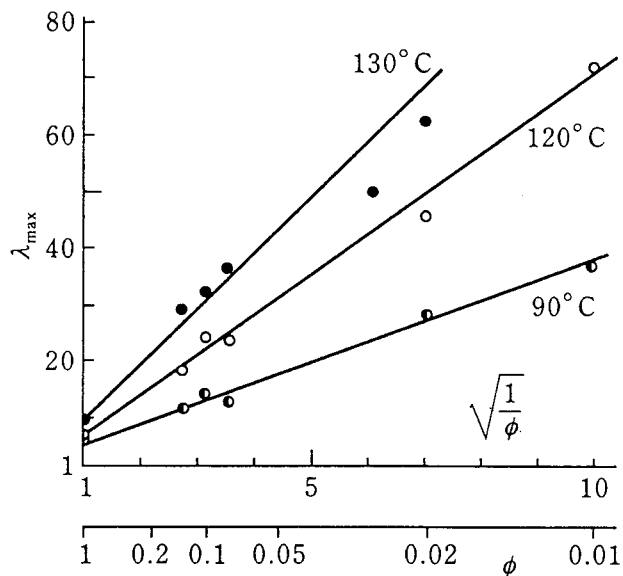


**Figure 17** Maximum draw ratio versus concentration of solution at various temperatures for PE.<sup>22</sup>



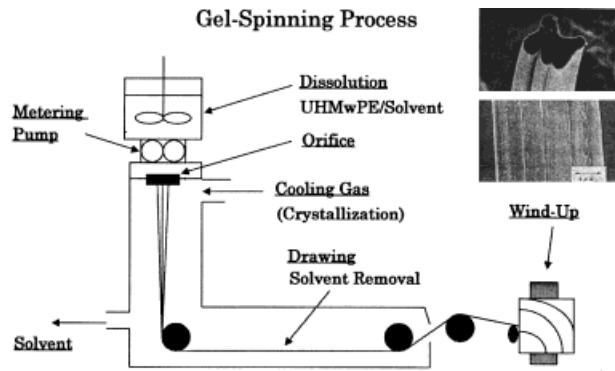


**Figure 18** Schematic illustration of gel spinning process of ultrahigh molecular weight PE.<sup>23</sup>

the single crystals, all of the molecules are aligned perpendicular to the mat surface. This mat can be drawn up to a draw ratio of about 100 and high-performance material can be prepared.<sup>19,20</sup> A similar concept was applied in the development of the two-stage drawing technique.<sup>21</sup> In this process, the polymer film is drawn to the transverse direction at first. In the drawn film, a lamella structure is formed, in that molecules are aligned in the drawing direction. High draw ratio can be achieved if the film is redrawn in the direction perpendicular to the direction of the molecular orientation.

Another important technique is the control of entanglement density by using a dilute solution. In the melt, it is not easy to control the entanglement density. However, entanglement density in solution varies in proportion to the concentration of polymer  $\phi$ . Since the maximum draw ratio is proportional to the square root of the number of segments, which is inversely proportional to the entanglement density, a plot of maximum draw

ratio versus  $(1/\phi)^{1/2}$  is expected to have a linear relation. Figure 17 shows the experimental result.<sup>22</sup> It also should be noted that there is a critical concentration at which entanglement of molecules begins to occur. This concentration (about 0.5 wt % in case of PE) is considered to be the optimum condition for the ultra drawing. If there is no entanglement in the solution, it is impossible to transfer tensile stress from one molecule to another. However, if there are too many entanglements, these remain in the drawn fibers and act as a defect, because the entanglements have a relatively long relaxation time.

## TECHNOLOGIES FOR THE PRODUCTION OF HIGH-PERFORMANCE FIBERS

### Gel Spinning of PE

One of the most successful technologies for the commercial production of high-performance fibers is the gel spinning and drawing of ultrahigh molecular weight PE. A schematic diagram of the gel spinning process is shown in Figure 18. In the spinning process, a carefully prepared solution is extruded from the orifice using a metering pump. By applying a cooling gas, crystallization of the extruded filaments occurs. Drawing is done along with the removal of the solvent. Obtained fibers do not have a circular cross-section, as shown in the inserted photographs.

Difficulties in the industrial production of high-performance fibers are summarized in Table II.<sup>23</sup> As shown in Figure 19, there is a hierarchy in the fiber structure, and for the production of high-performance fibers, all the micro-, submicro-, and macro-sized defects must be eliminated. In

**Table II Comparison of the Key Factors for Production of High-Performance Fibers in Laboratory Scale and Industrial Scale**

	Strategy Against Defects and Inhomogeneity	Laboratory Scale	Industrial Scale
Molecular weight	Chain-end ↓	$50\text{--}100 \times 10^4$	$100\text{--}1000 \times 10^4$
Concentration	Entanglement ↓	$C^*$ (ca. 0.5 wt %)	$C \gg C^*$
Drawing	Chain-folding ↓	Ultimate draw ratio in ideal (slow) drawing	Ultimate draw ratio High speed No fiber break
Number of Filaments	Difference between fibers ↓	Single filament	Multifilament (several thousands)
Attained strength		3–7 GPa	3–4 GPa

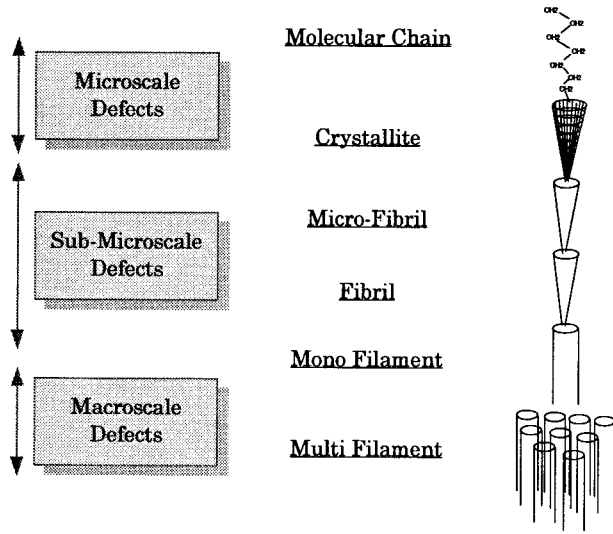


Figure 19 Hierarchy in fiber structure.<sup>23</sup>

fundamental research, methods for the removal of the micro-scale defects are mainly developed. For the industrialization of the process, macro-scale defects also should be avoided. Cost and quality are the crucial factors for the success of industrialization. Fiber processing conditions in laboratory scale and industrial scale productions are also compared in Table II. In the laboratory scale, the critical solution concentration can be adopted and drawing can be done at an idealized slow speed, whereas in the industrial scale, concentration should be increased and drawing speed should be increased to improve the productivity. Because several thousands of multifilaments are produced simultaneously in the industrial process, maintaining the evenness of the fibers both along the fiber direction and between fibers becomes very important.

Figure 20 shows the experimentally obtained unevenness of the high-strength PE fibers. There is an almost linear distribution of fiber strength

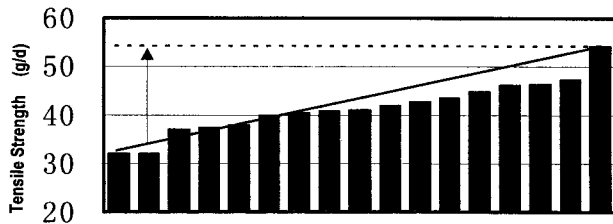


Figure 20 Strength distribution of high-strength PE fibers in a fiber bundle.

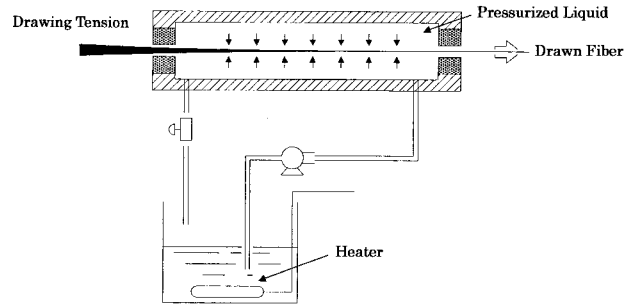


Figure 21 Pressurized drawing process for POM.

between 30 and 55 gf/d. This figure indicates that efforts for the elimination of unevenness surely lead to the improvement of overall fiber strength. In comparing the modulus and strength of various high-performance fibers, since PE has low density, the properties of the PE fibers become more prominent if the thickness of the fibers is expressed using linear density instead of cross-sectional area. From this point of view, it was reported that the PE fibers prepared by gel spin-

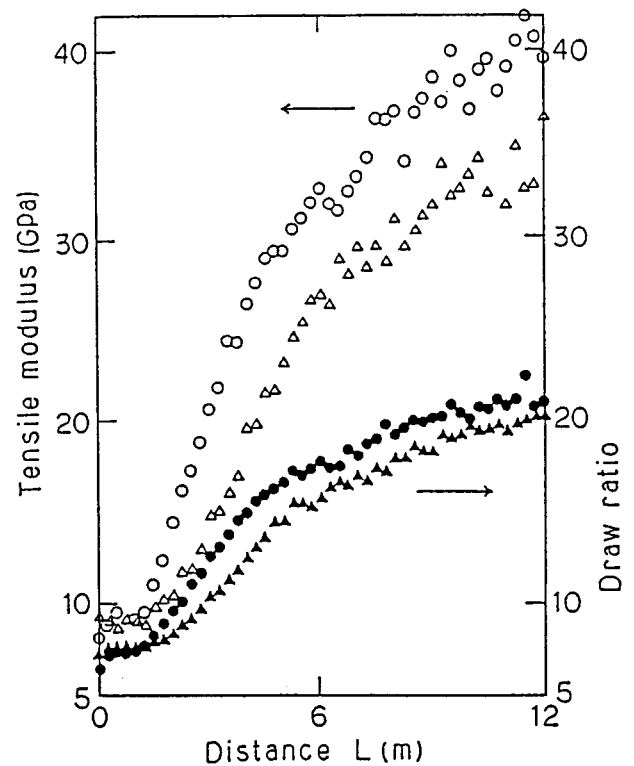


Figure 22 Effect of pressure on changes in draw ratio and tensile modulus of POM fibers in the vessel. Circles, with pressure; triangles, without pressure.<sup>24</sup>

ning process have superior mechanical properties than *p*-aramid fibers.

### Pressurized Drawing Process of Polyoxymethylene (POM)

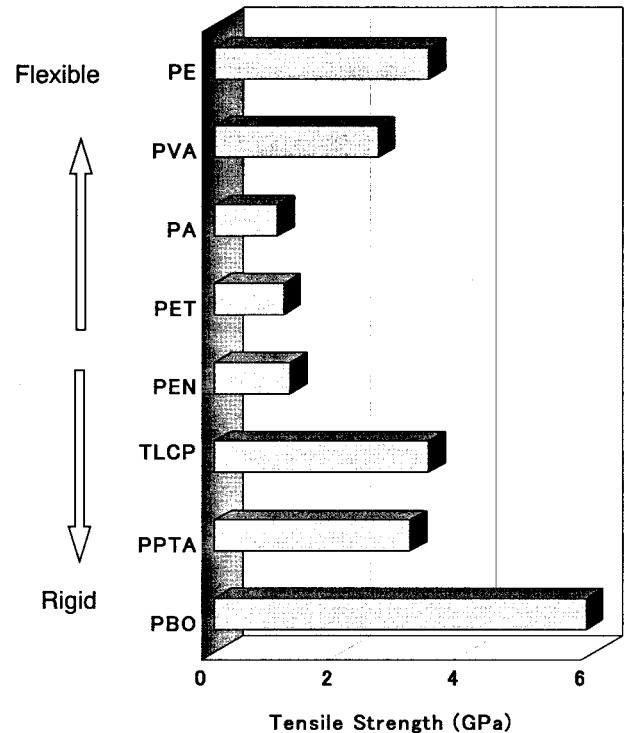
Pressurized drawing process<sup>24–26</sup> is being applied for the commercial production of high-performance POM fibers. The produced fibers are mainly used as geo-textiles. A schematic diagram of the pressurized drawing process is shown in Figure 21. The POM fiber is drawn in a vessel pressurized by heated liquid. The entrance and exit of the vessel are sealed to prevent the leakage of liquid. Experimental results for the production of high-performance POM fibers is reported, in that a hollow fiber with outer and inner diameters of 6.0 and 1.8 mm, respectively, is used as a starting material, and two stages of pressurized drawing are adopted. The liquid temperatures of the first and second drawing are 155 and 174°C, respectively.

Figure 22 shows the changes in draw ratio and tensile modulus of POM fibers in the vessel. The application of high pressure is reported to have the effects of reducing drawing stress and preventing the formation of micro-voids. Reduction of drawing stress reduces the possibility of fiber breakage in the drawing process, and the reduction of micro-voids improves the fiber properties. POM fibers with the tensile modulus of 50 GPa and tensile strength of 2 GPa can be produced in this process.

In the case of POM, drawing with the dielectric heating also is an effective way to improve the mechanical properties of the fibers.<sup>27</sup> It is explained that by the dielectric heating the amorphous part is selectively heated and eventually the efficiency of drawing can be improved.

### Controlled Drawing of PTFE

Processability of [poly(tetrafluoroethylene)] (PTFE) is very low because of its high viscosity and high melting temperature. Therefore, PTFE fibers are usually produced with the help of binding materials. It was reported recently that high-performance PTFE fibers with tensile modulus of 57.6 GPa and tensile strength of 2.31 GPa can be produced by a controlled drawing process in which a maximum draw ratio of 100 is attained.<sup>28,29</sup> In this process, a starting filament of 400- $\mu$ m diameter is produced by the paste extrusion of lubri-



**Figure 23** Attained strength of fibers prepared from various polymers.

cated PTFE powder. In the second stage, annealing of the starting filament is performed with a confined shrinkage, which is called sag. The annealing temperature is higher than the melting temperature of PTFE, 350°C. Observation under the polarizing microscope revealed that, at this temperature, the fiber maintains its optical anisotropy. During the annealing, the fiber shrinks. If the sag is less than 10%, fiber breakage occurs because of high shrinkage stress. At the sag of 25%, the fiber after the annealing shows a slightly tensioned state. If the sag is higher than 30%, the process can be regarded as the free-length annealing. It is reported that the cooling rate after the annealing process also is an important parameter for the drawability of fibers. Drawing was done at 388°C, which is also higher than the melting temperature of PTFE, and at the draw speed of 50 mm/s. It is considered that, during the annealing and cooling processes with the confined shrinkage, the entanglement structure changes and drawability can be improved under an optimum condition.

More recently, it was reported that by the application of a confined shrinkage process to knitted or woven partially oriented polyester fibers,

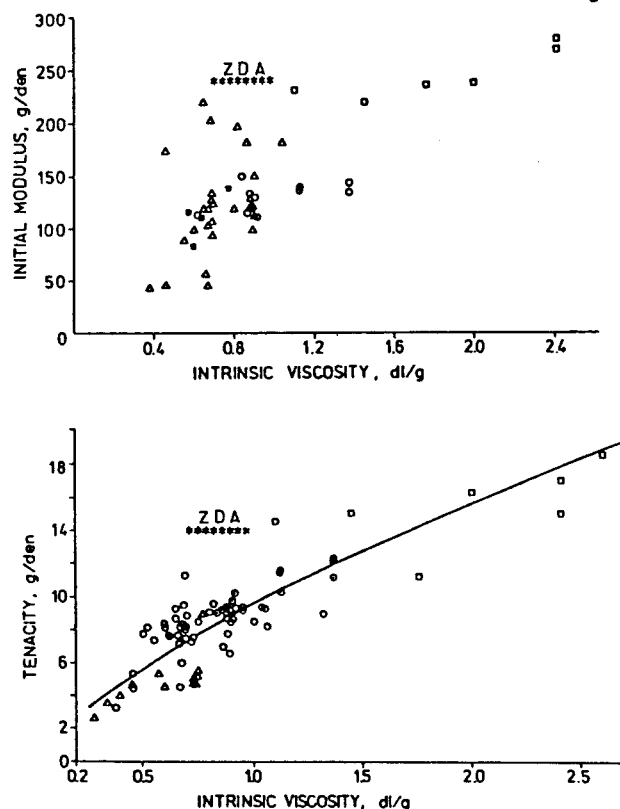


**Figure 24** Molecular weight dependence of modulus and tenacity of PET fibers. ZDA, zone drawing and annealing.

highly elastic polyester fabrics with good thermal stability are obtained.<sup>30</sup> In this process, PET fiber obtained at a take-up velocity of 3100 m/min was annealed at 180°C by confining the shrinkage. From the two results described above, the confined shrinkage process can be considered as a new processing technique for the production of some new types of fibers.

#### Solid State Co-Extrusion of High Molecular Weight PET

Production of high-performance fiber was accomplished through the gel spinning of flexible polymers and the spinning of rigid polymers utilizing a liquid crystalline state. However, the maximum mechanical properties obtained for PET, which have intermediate characteristics in terms of the rigidity of chain, still is quite low (Fig. 23). If we think of the domination of PET in the market, the improvement of the mechanical properties of PET is quite important.

The most effective approach for the production of PET fibers with improved mechanical properties so far is the utilization of high molecular weight polymers. High molecular weight PET can be obtained by solid-state polymerization. Because of extremely high viscosity, fiber formation of high molecular weight PET is usually accomplished by solution spinning or spinning with a plasticizer.<sup>31</sup>

Ito et al.<sup>32,33</sup> reported that the two-step drawing of solution-spun PET fibers with intrinsic viscosity of 3.6 dL/g leads to the formation of fibers with tensile modulus and strength of 39 and 2.3 GPa. Ziabicki<sup>34</sup> conducted a literature survey to summarize the effect of molecular weight on the mechanical properties of PET (Fig. 24). The improvement of mechanical properties of PET fibers by a controlled spinline process, in which liquid isothermal bath is set in the spinline, is reported by Cuculo et al.<sup>35</sup> and Lin et al.<sup>36</sup>

#### CONCLUSION

Basically there are two different approaches for the production of high-performance fibers. One is the development of a fiber formation process intending to obtain the ultimate mechanical properties without considering productivity. The other approach is the development of a process to improve fiber properties with a reasonable additional cost. In the latter case, if PET fibers with their tenacity, 100% higher than the conventional high-strength fibers, can be developed without any significant additional cost, the impact of the technology to the market is immeasurable. For this kind of technology, the control of entanglement in a molten state or in the undrawn yarn seems to be one of the most important factors.

The concept of entanglement has played a very important role in the development of high-performance fibers. However, the characterization of entanglement usually is done indirectly by utilizing some rheological or mechanical analysis. Therefore, the development of a method for the direct detection or accurate evaluation of entanglement is also an important future subject in this field.

The author is indebted to Mr. Yasuo Ohta of Toyobo Co. Ltd. for providing valuable suggestions on this subject.

## REFERENCES

1. Kunugi, T.; Ohta, T.; Yabuki, K. High-Strength High-Modulus Fibers; Kyoritsu Shuppan: Tokyo, Japan, 1988 (in Japanese).
2. Vincent, P. I. *Polymer* 1972, 13, 558.
3. Takeuchi, H.; Roe, R. J. *J Chem Phys* 1991, 97, 7458.
4. Tashiro, K.; Tadokoro, H. *Macromolecules* 1981, 14, 781.
5. Nishino, T.; Miyoshi, Y.; Nakamae, K. *Sen-i Gakkai Preprints* 1998, G-245.
6. Tashiro, K. *Sen-i Kikai Gakkaishi* 1995, 48, P425.
7. Termonia, Y.; Meakin, P.; Smith, P. *Macromolecules* 1985, 18, 2246.
8. Prevorsek, D. C. *Encyclopedia of Polymer Science and Technology*; Wiley Interscience: New York, 1993, p 803.
9. Smook, J.; Hamersma, W.; Pennings, A. J. *J Mater Sci* 1984, 19, 1359.
10. Nishino, T. *Kaigaikobunshikenkyu* 1996, 96, 70.
11. Tashiro, K.; Kobayashi, M.; Yabuki, K. *Kobunshi Ronbunshu* 1994, 51, 265.
12. Takahashi, T.; Tanaka, T.; Kamei, R.; Okui, N.; Takahiro, M.; Umemoto, S.; Sakai, T. *Kobunshi Ronbunshu* 1988, 45, 201.
13. Zwijnenburg, A. Ph.D. Thesis, University of Groningen: The Netherlands, 1978.
14. Okui, N.; Sakai, T. *Polym Bull* 1987, 16, 79.
15. Tashiro, K.; Tadokoro, H. *Macromolecules* 1981, 14, 781.
16. Arimoto, H. *J Polym Sci Pt A* 1964, 2, 2283.
17. Takahashi, A.; Ito, M.; Suzuki, K.; Kanamoto, T. *Sen-i Gakkai Preprints* 1998, G-12.
18. Pawlikowski, G. T.; Mitchell, D. J.; Porter, R. S. *J Polym Sci Pt B* 1988, 26, 1865.
19. Miyasaka, K.; et al. *J Polym Sci A-2*, 1969, 7, 2029.
20. Kunugi, T.; Oomori, S.; Mikami, S. *Polymer* 1988, 29, 814.
21. Kunugi, T. *Oriented Polymer Materials*; Huthig & Wepf: Heidelberg, Germany, 1996, p 304.
22. Smith, P.; Lemstra, P. J.; Booji, H. C. *J Polym Sci Phys* 1981, 19, 877.
23. Ohta, Y. *Sen-i Gakkaiishi* 1998, 54, P-8.
24. Komatsu, T.; Enoki, S.; Aoshima, A. *Polymer* 1991, 32, 1983.
25. Komatsu, T.; Enoki, S.; Aoshima, A. *Polymer* 1991, 32, 1988.
26. Komatsu, T.; Enoki, S.; Aoshima, A. *Polymer* 1991, 32, 1994.
27. Konaka, T.; Nakagawa, K.; Yamakawa, S. *Polymer* 1985, 26, 462.
28. Shimizu, M.; Ikeda, C.; Matsuo, M. *Macromolecules* 1996, 29, 6724.
29. Shimizu, M. U. S. Pat. 5,686,833, 1997.
30. Taguchi, S.; Okamoto, M. *Jpn. Pat. Appl.*, 96-283437.
31. Tate, S.; Chiba, S.; Tani, K. *Polymer* 1996, 37, 4421.
32. Ito, M.; Wakayama, Y.; Kanamoto, T. *Sen-i Gakkaishi* 1992, 48, 569.
33. Huang, B.; Ito, M.; Kanamoto, T. *Polymer* 1994, 35, 1210.
34. Ziabicki, A. *Text Res J* 1996, 66, 705.
35. Cuculo, J. A.; Tucker, P. A.; Chen, G.-Y. *J Appl Polym Sci Appl Polym Symp* 1991, 47, 223.
36. Lin, C.-Y.; Tucker, P. A.; Cuculo, J. A. *J Appl Polym Sci* 1992, 46, 531.